First-principles calculations of β-SiC(001) surfaces

M. Sabisch, P. Krüger, A. Mazur, M. Rohlfing, and J. Pollmann
Institut für Theoretische Physik II, Universität Münster, D-48149 Münster, Germany
(Received 10 November 1995; revised manuscript received 17 January 1996)

We report self-consistent *ab initio* calculations of structural and electronic properties for five different configurations of polar β-SiC(001) surfaces. Both Si- and C-terminated structures are investigated. We employ our smooth norm-conserving pseudopotentials in separable form within the local-density approximation of density-functional theory. Gaussian orbital basis sets are used in the supercell calculations. For the Si-terminated (2×1) surface we do not find any significant dimerization of the surface-layer Si atoms. For various C-terminated surfaces, on the contrary, we find strong carbon dimers as the basic building blocks of the reconstruction. Our optimized configurations for C-terminated surfaces are in good general agreement with structural models from the literature that have been suggested on the basis of experimental data. Our results for the Si-terminated (2×1) surface, on the contrary, show significant differences from suggested models. We discuss the physical origins of the distinctly different reconstruction behavior of Si- and C-terminated surfaces and present a full account of surface electronic properties of these systems including the quasiparticle band structure of the C-terminated β-SiC(001)-(2×1) surface as resulting in the *GW* approximation. We present and discuss our results in comparison with other theoretical results and with experimental data from the literature. [S0163-1829(96)04319-6]

I. INTRODUCTION

The large technological potential of SiC for electronic devices[1–3] has led to a strong current interest in its bulk and surface properties in both experiment and theory. From a more fundamental point of view, SiC is an extremely intriguing group-IV semiconductor since many of its properties can be expected to be related to those of diamond and Si in interesting ways. While these elemental semiconductors exhibit only one stable phase at room temperature, the compound semiconductor SiC exists in very many polytypes. A lot of interest in experiment and theory has been concentrated on the hexagonal α phases and on the cubic β phase. Cubic β-SiC has one Si and one C atom per bulk unit cell. Although a group-IV semiconductor, SiC exhibits a relatively large ionicity of $g=0.475$ on the Garcia-Cohen scale,[4] as discussed in detail, e.g., in Ref. 5. The heteropolarity of the SiC bond stems from the very different strengths of the C and Si potentials giving rise to very different covalent radii $r_c^{\mathrm{C}}=0.77$ Å and $r_c^{\mathrm{Si}}=1.17$ Å, respectively. Correspondingly, the electronegativity of C ($e_{\mathrm{C}}=2.5$) is considerably larger than that of Si ($e_{\mathrm{Si}}=1.7$). The stronger C potential, as compared to that of Si, leads to a charge transfer $\delta\rho_{\mathrm{Si}\rightarrow\mathrm{C}}$ from Si to C so that the electronic charge density distribution about the midpoint of the Si-C bond is strongly asymmetric (see, e.g., Figs. 4 and 5 of Ref. 5). In consequence, Si atoms act as cations while C atoms act as anions in β-SiC and its (001) surfaces are polar. Si and C layers alternate with a distance of $a_0/4$ along the (001) direction, a_0 being the SiC bulk lattice constant. Thus there are two types of distinctly different polar β-SiC(001) surfaces, namely, Si- or C-terminated (001) surfaces.

A large variety of reconstructions of these surfaces has been observed in experiment.[6–13] They have been investigated by low-energy electron diffraction (LEED),[6–13] Auger electron spectroscopy (AES),[6–13] and electron energy loss spectroscopy (EELS).[6,7,9] In addition, x-ray photoelectron and ultraviolet photoelectron spectroscopy,[9] medium-energy ion scattering (MEIS),[8] and scanning tunneling microscopy (STM) studies[13] have been carried out. Among the structures reported are (1×1), (2×1), $c(2\times2)$, $c(4\times2)$, (3×2), (5×2), and (7×2). For these reconstructions a number of models have been proposed. Since their discovery by Dayan,[6] Si-terminated surfaces have been modeled by ordered arrays of surface Si dimers.[6–9,12,13] Dayan suggested a $c(2\times2)$ staggered array of Si dimers.[6] For the Si-terminated (2×1) reconstruction, Powers *et al.*[12] arrived on the basis of their tensor LEED analysis at a model consisting of Si dimer rows with a dimer bond length of 2.31 Å very similar to that of the Si(001)-(2×1) surface. Hara *et al.*[13] studied Si adlayers at the Si-terminated surface, formed by *in situ* cleaning, employing LEED and STM. They observed (3×2), (5×2), and (7×2) reconstructions. The C-terminated surface was investigated in detail, e.g., by Bermudez and Kaplan,[10] as well as by Powers *et al.*[11] Both groups prepared C-terminated surfaces by two different methods. In one method, surface Si atoms were removed from the (2×1) surface by high-temperature annealing in ultrahigh vacuum, while in the other C was deposited by exposing the stoichiometric (2×1) surface at 800–1100 or at 1125 K, respectively, to C_2H_4. In both cases the authors obtained very similar ordered $c(2\times2)$ structures which turned out to be more uniform and well ordered when the second preparation method was employed. Bermudez and Kaplan[10] proposed a $c(2\times2)$ structure for this surface, resembling the staggered dimer model suggested by Dayan[6] for the Si-terminated surface. In contrast, Powers *et al.*[11] favored a $c(2\times2)$ structure with C_2 groups in staggered silicon bridge sites. Their tensor LEED calculations showed no significant differences from the conventional dynamical LEED results for the staggered carbon dimer model suggested by Bermudez and Kaplan.[10]

The optimized R factors for the latter model, however, were found to be significantly larger than those for the bridging C_2 group model.[11] In several of the experimental investigations it was observed that the spectra of one particular surface phase frequently showed weak features associated with other phases, since several of the possible β-SiC(001) reconstructions can exist on the surface simultaneously, depending on the local atomic composition.[10,11] It was concluded,[10–12] therefore, that a full understanding of the mechanisms driving the reconstructions at the polar SiC(001) surfaces must await detailed total-energy studies. The purpose of our contribution is to report the results of such studies for a number of conceivable surface reconstructions.

Ab initio results for various different SiC(001) surfaces have recently been reported by Yan, Smith, and Jónsson,[14] by Käckell, Furthmüller, and Bechstedt,[15] and by our group.[16] Semiempirical structure studies of (001) surfaces have been reported by Craig and Smith,[17,18] by Mehandru and Anderson,[19] and by Badziag.[20]

In this paper we present and discuss the results of our *ab initio* pseudopotential calculations carried out within the local-density approximation (LDA). A preliminary account of these results is included in a recent review article on structural and electronic properties of prototype surfaces of group-IV, III-V, and II-VI semiconductors.[16] We have studied five different configurations of polar β-SiC(001) surfaces using smooth pseudopotentials and localized Gaussian orbital basis sets. The calculations have been carried out within the supercell approach. For the Si-terminated surface we have considered only the (2×1) reconstruction, while for the C-terminated surface, we have considered a (2×1), a (1×2), and two $c(2\times2)$ reconstructions containing dimers of C_2 groups in row or staggered configurations, respectively. We present optimal reconstruction configurations and the respective surface electronic structures. In particular, we address the question to what extent the reconstructions of the SiC(001) surfaces are similar to or distinctly different from those of the related C(001) and Si(001) surfaces.

The paper is organized as follows. In Sec. II we briefly summarize the framework of our calculations. In Sec. III we present and discuss our results for the Si-terminated (2×1) and for four different configurations of the C-terminated β-SiC(001) surface. The latter were found to be relatively close local minima of the total energy in configuration space. All our results are compared with those of other calculations and with available experimental data. A summary concludes the paper in Sec. IV.

II. CALCULATIONAL FRAMEWORK

The calculations are carried out in the framework of density-functional theory (DFT) using the local-density approximation.[21] For the exchange and correlation potential we employ the functional of Ceperley and Alder[22] as parametrized by Perdew and Zunger.[23] We use nonlocal, norm-conserving pseudopotentials in the separable form, as suggested by Kleinman and Bylander.[24] These pseudopotentials have been reported elsewhere.[25] They were generated following the prescription given by Hamann, Schlüter, and Chiang.[26] Employing our very smooth pseudopotentials, the numerical effort is strongly reduced. This is of particular importance because of the presence of carbon which is a second-row element. In contrast to previous calculations which have employed plane waves, we express the wave functions in terms of linear combinations of Gaussian orbitals with s, p, d, and s^* symmetry. We have found that 30 Gaussians per surface-layer atom and 20 Gaussians per atom for all other atoms in the supercell yield sufficient accuracy.[5] The decay constants for Si are 0.2 and 0.6 (at the surface 0.18, 0.5, and 1.0). For the C atoms we use 0.35 and 1.7 (at the surface 0.25, 1.0, and 2.86). All constants are given in atomic units. Using these pseudopotentials and Gaussian orbitals yields results for bulk β-SiC which are in excellent agreement with the results of converged plane-wave calculations and with experimental data, as we have shown previously.[5] With this approach we have successfully investigated the β-SiC(110)-(1×1) surface, as well.[5] The total energy is calculated self-consistently using the momentum-space formalism of Ihm, Zunger, and Cohen.[27] All computations are performed using sets of eight $\mathbf{k}_\parallel$ points for the (2×1) unit cell and four $\mathbf{k}_\parallel$ points for the $c(2\times2)$ unit cell, in the irreducible part of the surface Brillouin zone (SBZ). This number of $\mathbf{k}_\parallel$ points turned out to be important for good convergence. The total energies of the different investigated geometries of C-terminated (001) surfaces were all calculated on equal footing in a (2×2) unit cell with four $\mathbf{k}_\parallel$ points in the irreducible part of the SBZ, to allow for a more meaningful comparison of the reconstruction-induced energy gains.

The optimal surface configuration is determined within the supercell approach. In our calculations we employ eight layers of SiC, one hydrogen, and seven vacuum layers in the supercell. The lower four atomic layers were fixed in the bulk configuration with the theoretical lattice constant of 4.34 Å. The broken sp^3 bonds at the atoms on the bottom layer were saturated with hydrogen in fixed positions to avoid electronic states in the gap energy region that originate from these bonds. The optimal surface geometry was determined by successive elimination of the forces using the Broyden scheme.[28] In addition to the Hellmann-Feynman forces, Pulay forces had to be taken into account because of the use of Gaussian orbital basis sets.[29] We move the atoms of the upper four layers in the supercell until all forces vanish within 10^{-3} Ry/a.u.

III. POLAR SURFACES OF β-SiC(001)

Considering Si- or C-terminated (001) surfaces of β-SiC, one might expect that they show a reconstruction behavior very similar to the respective Si(001)-(2×1) and C(001)-(2×1) surfaces, i.e., an asymmetric dimer reconstruction for the former and a symmetric dimer reconstruction for the latter (see, e.g., Refs. 16 and 30). As a matter of fact, experimental data have been interpreted on the basis of this expectation, since there were no *ab initio* total-energy calculations for polar β-SiC surfaces available at the time. It was concluded that the LEED results for the Si-terminated (2×1) surface indicate that the surface is terminated by a layer of Si atoms forming asymmetric, buckled dimer rows.[12] For the C-terminated surface various models based on symmetric C dimers have been proposed.[10,11] Considering the reconstruction of polar β-SiC(001) surfaces in comparison

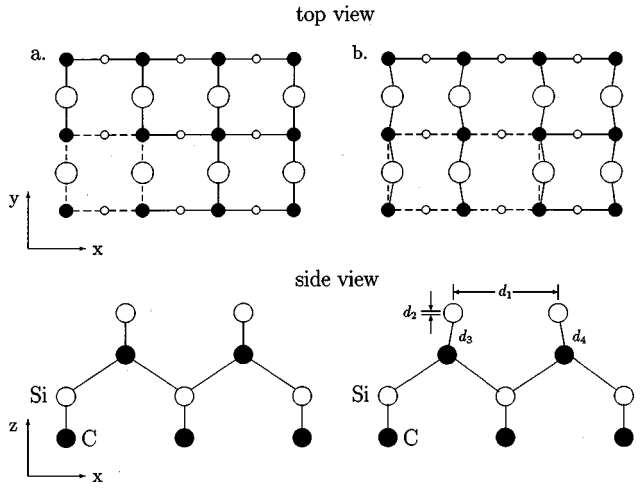

FIG. 1. Top and side views of the ideal (a) and the (2×1)-reconstructed (b) configurations of the Si-terminated β-SiC(001) surface. In this and in all following figures related to the surface structure, Si atoms are represented by open circles while C atoms are represented by black dots. Unit cells are shown by dashed lines and the labeling of characteristic structural parameters is introduced. The vertical distance between the two top-layer Si atoms at the reconstructed surface is labeled d_2.

with the respective Si and diamond surfaces, one should bear in mind, however, that the bulk charge densities and the lattice constants of these three semiconductors are considerably different (see, e.g., Ref. 5). The valence charge is $4e$ in both Si and diamond, while it is $3.86e$ at the Si cations and $4.14e$ at the C anions in β-SiC, as we have obtained from a Mulliken analysis. Thus a charge transfer of $\delta\rho_{\mathrm{Si}\rightarrow\mathrm{C}}=0.14e$ results from our calculations. The experimental (our theoretical) lattice constants a_0 of 3.57 (3.52) Å for diamond, 4.36 (4.34) Å for β-SiC, and 5.43 (5.38) Å for Si show that the lattice constant of β-SiC is 22% larger than that of diamond but 20% smaller than that of Si. These differences in charge densities and lattice constants have some bearing on the reconstruction behavior of β-SiC(001), as compared to C(001) and Si(001), respectively.

A. The Si-terminated β-SiC(001)-(2×1) surface

Experimental data indicate that the Si-terminated β-SiC(001) surface shows (2×1), $c(4\times2)$, (3×2), and (5×2) reconstructions.[6–9,12,13] We have concentrated on the (2×1) configuration to keep the numerical effort manageable. We first present our optimal surface structure. Next we address the related electronic structure. In a third subsection we compare our results with literature data. Finally, we compare the structural and electronic properties of the Si-terminated β-SiC(001)-(2×1) with those of the Si(001)-(2×1) surface.

1. Surface structure

The optimized geometry resulting from our self-consistent calculations is shown by a top and a side view in Fig. 1 in comparison with the structure of the ideal (001) surface. In our structure optimizations we have relaxed the atoms on the first four layers in x and z directions (see Fig. 1). At the ideal surface, the Si surface-layer atoms reside at a distance of 3.08 Å. In our calculated optimal structure they move slightly towards each other and their distance d_1 amounts to 2.73 Å. *No Si surface dimers are formed* in striking contrast to the Si(001)-(2×1) surface. The observed distance of 2.73 Å between the Si surface-layer atoms at the β-SiC(001)-(2×1) surface is much larger than the dimer bond length of 2.25 Å at the Si(001)-(2×1) surface (see, e.g., Refs. 30–32). The energy gain due to the reconstruction is extremely small, amounting to 0.01 eV per unit cell only. In Table I we compile our structural parameters for the optimized geometry together with previous results from the literature. Before we discuss these results in comparison let us first address the electronic structure of this surface.

2. Surface electronic structure

The surface electronic structure of the ideal and of our optimally reconstructed Si-terminated β-SiC(001)-(2×1) configuration is shown in the upper two panels on the left-hand side of Fig. 2 together with the projected band structure (PBS) of bulk SiC. The PBS has a direct gap of 1.28 eV which is smaller than the experimental gap of 2.41 eV. This is due to the well-known underestimate of the gap energy in the LDA. The surface band structure of the ideal surface has been backfolded onto the (2×1) SBZ for a more meaningful comparison. At the ideal surface, we find a dangling-bond band D and a bridge-bond band Br in the gap energy region (actually there are two bands in each case due to the back-

TABLE I. Calculated structure parameters for the Si-terminated β-SiC(001)-(2×1) surface (for their definition, see Fig. 1) as resulting from our work in comparison with other theoretical results and experimental data from the literature. The values of Ref. 14 were obtained employing a (2×2) configuration.

Si-terminated (2×1)	This work	Käckell *et al.* [a]	Yan *et al.* [b]	Craig and Smith [c]	Mehandru and Anderson [d]	Powers *et al.* [e]
d_1 (Å)	2.73	2.75	2.26	2.33	2.16	2.31
d_2 (Å)	0.00	0.00	0.05	0.20		0.20
d_3 (Å)	1.89			1.78		
d_4 (Å)	1.89			1.85		

[a]Reference 15.
[b]Reference 14.
[c]Reference 17.
[d]Reference 19.
[e]Reference 12.

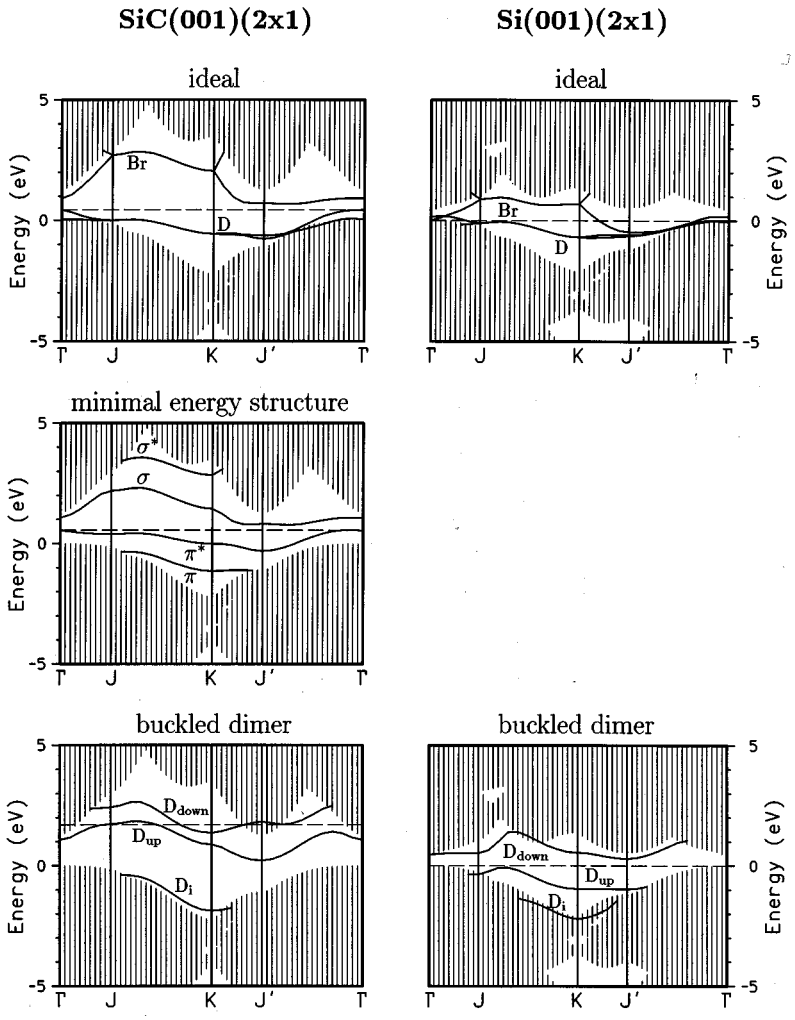

FIG. 2. Sections of the electronic structure of ideal and reconstructed Si-terminated β-SiC(001)-(2×1) as well as Si(001)-(2×1) surfaces for comparison. Note that the minimal-energy structure is a buckled dimer configuration in the case of Si(001)-(2×1) but not in the case of Si-terminated β-SiC(001)-(2×1). For further comparison a corresponding section of the surface band structure of the Si-terminated SiC(001)-(2×1) surface in a buckled dimer configuration is shown in the lower left panel (for details, see text). High-symmetry points are labeled as usual. The projected band structure of the bulk crystal is shown by vertically shaded areas.

folding). They are very similar, in general, to the well-known *D* and Br bands at the ideal Si(001) surface whose band structure is shown in the upper right panel of Fig. 2 for comparison, as well. The reconstruction of the β-SiC(001) surface reduces the symmetry, giving rise to corresponding shifts and splittings of the former *D* and Br bands. Four new bands (π, π^*, σ, and σ^*) result (see middle panel of Fig. 2). Note that, e.g., the dispersion of the σ band is very similar to that of the lower branch of the Br band at the ideal surface. A strong splitting of the twofold-degenerate Br band between *J* and *K* gives rise to the bands σ and σ^*. Very similar behavior concerning the *D* bands at the ideal surface, splitting into a π and a π^* band, is to be observed in the middle panel of Fig. 2. In consequence of the reconstruction, the four individual bands significantly differ from the *D* and Br bands at the ideal surface but their center of gravity hardly changes. In consequence, only a very small total-energy gain of $E_{\mathrm{rec}}=10$ meV results. The gap of the reconstructed surface is virtually the same as that of the ideal surface.

The nature and origin of the four new bands at the reconstructed surface become apparent from Fig. 3 where we show charge densities of the related states at the *K* point of the surface Brillouin zone. The occupied states π and π^* mainly result from symmetric and antisymmetric combinations of the former dangling-bond orbitals, while the empty states σ and σ^* result from symmetric and antisymmetric combinations of the former bridge-bond orbitals. Since the *D* bands at the ideal surface originate from *s* and p_z wave functions and the Br bands at the ideal surface originate predominantly from p_x orbitals, the resulting π and π^* bands at the reconstructed surface are lower in energy than the σ and σ^* bands, amazingly enough.

3. Comparison with literature data

Our optimized structure for the Si-terminated β-SiC(001)-(2×1) surface is in good agreement with the theoretical results of Ref. 15 but in marked contrast to the theoretical results of Refs. 17 and 18 and the experimental results of Ref. 12 (see Table I). The *ab initio* LDA calculation by Käckell, Furthmüller, and Bechstedt[15] using plane-wave basis sets and smooth Troullier-Martins pseudopotentials yields an optimal distance of the symmetrically displaced Si surface-layer atoms of $d_1=2.75$ Å and an energy gain of roughly 0.01 eV per surface unit cell, in very close agreement with our results. On the contrary, the empirical calculations of Craig and Smith[17] yield Si surface dimers with a dimer bond length of $d_1=2.33$ Å and a buckling of $d_2=0.20$ Å. Si surface dimers with a small bond length of $d_1=2.26$ Å and a dimer buckling of $d_2=0.05$ Å have been obtained, as well, in the very recent *ab initio* study

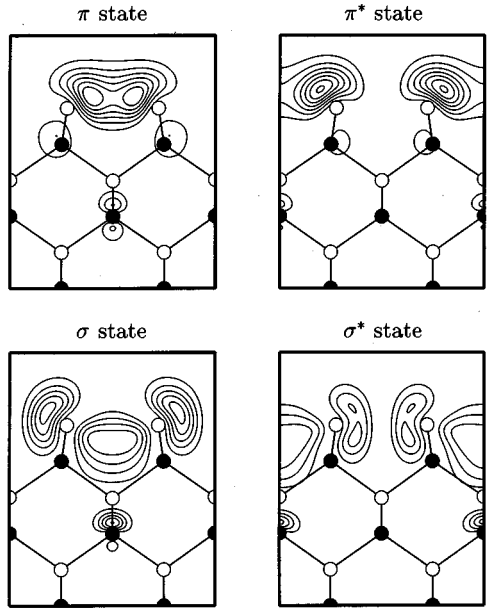

FIG. 3. Charge density contours of salient surface states at the K point of the (2×1) SBZ of the Si-terminated β-SiC(001)-(2×1) surface shown in the x-z plane containing the Si surface atoms. All atoms are connected by solid lines also if the indicated bonds do not lie in the plane of the drawing.

by Yan, Smith, and Jónsson[14] carried out for a (2×2) configuration. Actually, our calculations show that the total-energy curve as a function of the reconstruction is very flat. Thus a correct description of the reconstruction-induced charge density relaxations is very demanding. It seems that the empirical approach employed by Craig and Smith[17] may not be precise enough to take such sensitive effects quantitatively into account. At the same time, it appears that the $\mathbf{k}_{\parallel}$-point sampling employed by Yan and co-workers[14,33] in their *ab initio* calculations is responsible for their particular results. Actually, these authors carried out calculations for a (2×2) unit cell using only the $\Gamma_{2\times2}$ point of the SBZ in their $\mathbf{k}_{\parallel}$-point sampling.[33] We think that the different optimal structures resulting in Ref. 14 and in our work are due to different $\mathbf{k}_{\parallel}$-point samplings. To corroborate our conjecture, we have carried out two additional sets of calculations. First we have considered a fully buckled dimer configuration, using a dimer bond length of $d_1=2.27$ Å and a dimer buckling of $d_2=0.20$ Å (these values are close to those of Refs. 12, 14, and 17) and have calculated its surface electronic structure and its total energy employing our usual mesh with $8\mathbf{k}_{\parallel}$ points in the irreducible part of the (2×1) SBZ. The resulting surface band structure for this configuration is shown in the lower left panel of Fig. 2. The surface turns out to be strongly metallic in this configuration. The resulting occupied $D_{\rm up}$ band resides much higher in energy than the occupied π^* band in the middle panel of Fig. 2. The total energy of this fully buckled dimer configuration is 0.67 eV *higher* than that of our optimized geometry. This result rules out a full asymmetric dimer reconstruction of the Si-terminated β-SiC(001)-(2×1) surface. Second, we have carried out structure optimization calculations using only the $\Gamma_{2\times1}$ and the $J'_{2\times1}$ points of the (2×1) SBZ, which corresponds to taking only the $\Gamma_{2\times2}$ point in the (2×2) SBZ. Actually, in this case we arrive at virtually the same geometry as that of Yan, Smith, and Jónsson.[14] If only these high-symmetry points are used, it is obvious from the surface band structure in the lower left panel of Fig. 2 that such calculations mimic a semiconducting surface, although it is strongly metallic. The small number of only two high-symmetry $\mathbf{k}_{\parallel}$ points probably does not allow one to take the related charge density relaxations properly into account. Smith and Jónsson[33] have extended their calculations in the meantime to a number of different configurations and have confirmed that the total-energy curve of the Si-terminated β-SiC(001)-(2×1) surface is indeed very flat and has to be studied with extreme care.

Powers *et al.*[12] have interpreted their tensor LEED data as indicating that buckled dimers with a dimer bond length of $d_1=2.31$ Å and a dimer buckling of $d_2=0.20$ Å are formed. One could imagine that the expectation of a buckled dimerization has biased the analysis towards the final result in view of the reconstruction of the Si(001)-(2×1) surface. Our optimized structure cannot be reconciled with the data, as far as the two top layers of the surface are concerned. On the contrary, our calculated atomic displacements on the lower-lying sublayers, which are less than or equal to 0.02 Å, are in good agreement with the sublayer-atom displacements derived by Powers *et al.*[12] from their tensor LEED data.

It has been argued that an additional Si layer adsorbed on top of the Si-terminated SiC(001)-(2×1) surface could be responsible for the experimentally observed dimerization. To confirm or disprove this conjecture we have added one monolayer of Si to our Si-terminated surface system and optimized its structures anew. In this case also, we observe only slight displacements of the top-layer Si atoms with a surface bond length of $d_1=2.68$ Å. In a similar calculation Käckell, Furthmüller, and Bechstedt[15] obtained a bond length of $d_1=2.55$ Å in the added Si layer, again with no full dimerization. This value is smaller than ours but it is still far away from the value of $d_1=2.31$ Å quoted from experiment.[12] The backbond lengths increase in this case to 2.50 Å in our results and to 2.49 Å in the result of Ref. 15, as compared to the backbond lengths of 2.28 and 2.33 Å at the Si(001)-(2×1) surface,[30] strongly emphasizing the differences between the two structures, originating from the charge transfer in SiC and from the smaller lattice constant of β-SiC as compared to Si.

4. Comparison with Si(001)-(2×1)

Our optimized structure of the Si-terminated β-SiC(001)-(2×1) surface significantly differs from that of the Si(001)-(2×1) surface, which shows an asymmetric dimer reconstruction (see Fig. 4 for a direct comparison). The origins of the different reconstruction behavior of these two surfaces can partly be seen in Fig. 2, in which we have also included the surface band structure for the optimally dimerized[30–32] Si(001)-(2×1) surface (see lower right panel).

Comparing the two top panels of Fig. 2, we recognize that the ideal Si-terminated β-SiC(001) surface is already semiconducting while the ideal Si(001) surface is metallic. In addition, the calculated gap of SiC ($E_g=1.28$ eV) is much larger than the calculated gap of Si ($E_g=0.56$ eV). Both results are related to the fact that the C potential is stronger

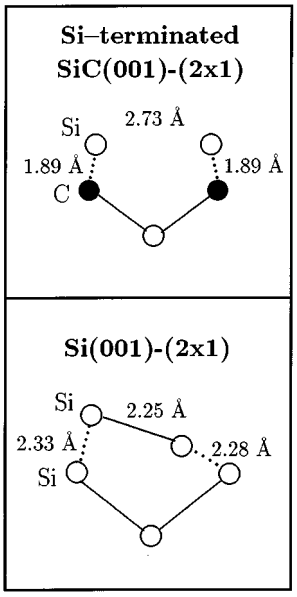

FIG. 4. Side view of the basic building block of the optimized configuration of Si-terminated β-SiC(001)-(2×1), as obtained in this work. For a direct comparison the related side view of the Si(001)-(2×1) surface, as reported in Ref. 30, is given as well. Bonds lying in or parallel to the plane of drawing are indicated by full lines. Bonds which form an angle with the plane of drawing are shown by dotted lines. The distance of 2.73 Å between surface-layer Si atoms in our optimized β-SiC(001)-(2×1) configuration is much larger than, e.g., the Si bulk bond length of 2.35 Å, so that we have not indicated a *bond* between the two surface-layer atoms in the top panel by a full line.

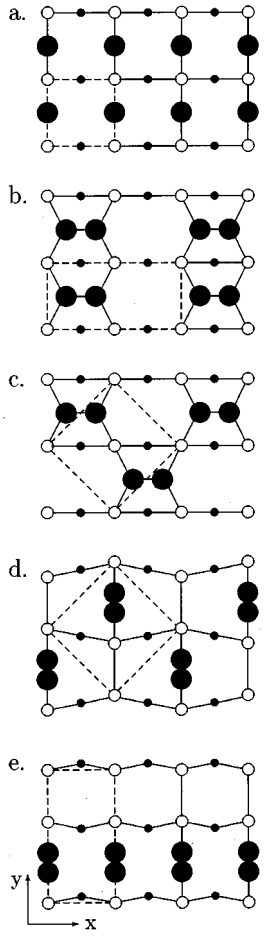

FIG. 5. Top views of the ideal (a) and four different reconstructed C-terminated surfaces (b)–(e) of β-SiC(001). All four reconstructed configurations are local minima of the total energy. In our results the (2×1) dimer row reconstruction (b) is the absolute minimum configuration relative to the $c(2\times2)$ staggered dimer configuration (c), the $c(2\times2)$ staggered C_2 group configuration (d), and the (1×2) C_2 group row configuration (e). The unit cells are indicated by dashed lines.

than the Si potential. In consequence, the C potentials at the second layer of Si-terminated β-SiC(001)-(2×1) cause the s,p_z-type dangling-bond bands D to be lower in energy with respect to the p_x-type bridge-bond bands Br at this surface than at the Si(001) surface, which has Si atoms in the second layer, of course. Therefore a strong reconstruction is needed at Si(001) to make this surface semiconducting (see lower right panel of Fig. 2), in agreement with experiment. The formation of fully buckled dimers at Si(001)-(2×1) leads to an energy gain of $E_{\mathrm{rec}}=1.94$ eV per unit cell.[30] On the contrary, there is no need for such a pronounced structural transition at the Si-terminated β-SiC(001) surface because it is semiconducting already in its ideal configuration. Consequently, the band structure of our optimized structure (see top panel of Fig. 4) remains semiconducting (see middle panel of Fig. 2). A fully buckled dimer configuration of this surface is strongly metallic (see lower left panel of Fig. 2) and the related total energy is 0.67 eV higher than that of our optimized configuration.

In addition, the charge transfer between Si and C in β-SiC as well as the considerably smaller lattice constant of β-SiC as compared to Si have some influence on the different reconstruction behavior of the two surfaces. Furthermore, when surface dimers are to be formed at (001) surfaces, angular forces on the second-layer atoms are involved. These are considerably larger for C than for Si. It is thus easier to form Si dimers at the Si(001) surface than at the Si-terminated β-SiC(001) surface.

B. The C-terminated β-SiC(001) surface

A number of structural models for the C-terminated β-SiC(001) surface have been suggested on the basis of experimental results. In Fig. 5 we have compiled the structures studied in this work. A $c(2\times2)$ reconstruction[8,10,11] has been observed experimentally for the SiC(001) surface terminated by a full monolayer of carbon. One model geometry for that surface has been proposed by Bermudez and Kaplan,[10] who suggested a staggered arrangement of C dimers [see Fig. 5(c)]. A C dimer row structure is shown in Fig. 5(b). Another model proposed by Powers *et al.*[11] consists of C_2 groups in bridge positions above the Si sublayer atoms. These C_2 groups are supposed to form a staggered arrangement,[11] as shown in Fig. 5(d). We have considered (2×1) C dimer row and (1×2) C_2 group row as well as $c(2\times2)$ staggered dimer and staggered C_2 group reconstructions. The resulting optimal structures obtained from our total-energy minimization are shown in Figs. 5(b)–5(e). The total energies for all these structures have been calculated in a (2×2) unit cell for a more meaningful comparison.

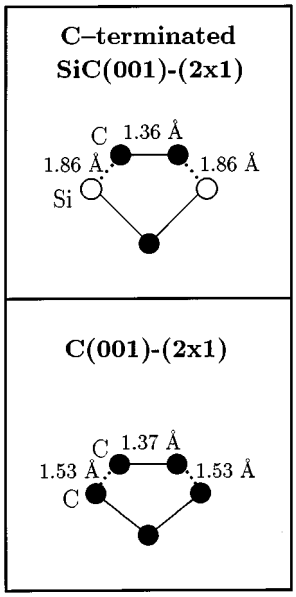

FIG. 6. Side view of the optimal C-terminated dimer row reconstruction of β-SiC(001)-(2×1), as determined in this work, in direct comparison with the related structure of C(001)-(2×1), as reported in Ref. 30. The bonds are indicated as in Fig. 4.

1. (2×1) dimer row structure

First we have optimized the (2×1) dimer row reconstruction of the C-terminated β-SiC(001) surface [see Fig. 5(b)]. The atoms on the first four layers in the supercell were allowed to move in the *x*-*z* plane. As the minimum-energy configuration we obtain symmetric C dimers in the surface layer with a bond length of 1.36 Å. The dimers form C═C double bonds very similar to those in the C_2H_4 molecule or at the C(001)-(2×1) surface, where they have a bond length of 1.34 (Ref. 34) or 1.37 Å,[30] respectively. The reconstruction of this C-terminated SiC(001)-(2×1) surface turns out to be extremely similar to that of the C(001)-(2×1) surface (see Fig. 6). The arguments given in Sec. III A 4 against dimer formation at Si-terminated β-SiC(001)-(2×1) now work in favor of dimerization at the C-terminated β-SiC(001)-(2×1). The charge transfer increases the charge at the C anions, the lattice constant of β-SiC is 20% larger than that of diamond, and the angular forces on the second-layer Si atoms of this surface are comparatively smaller. The energy gain due to this (2×1) C dimer row reconstruction is $E_{\rm rec}=4.88$ eV per (2×1) unit cell. This energy gain is considerably larger than the energy gain of $E_{\rm rec}=3.36$ eV at the C(001)-(2×1) surface,[30] in spite of the fact that the C═C dimer double-bond length is almost identical in both cases (see Fig. 6 for the matter). This increase in energy gain at the C-terminated β-SiC(001)-(2×1) surface, as compared to C(001)-(2×1), should largely be due to the charge transfer from Si to C in β-SiC and to the larger lattice constant of β-SiC as compared to diamond. We mention already at this point that the (2×1) dimer row structure results as the minimum-energy configuration of all four structures which we have considered.

Table II shows our optimal structure parameters for this configuration in comparison with theoretical results from the literature. In this case of a very strong reconstruction our results and those of Craig and Smith[18] turn out to be identical. It seems that the calculation of the very steep total-energy minimum that characterizes this reconstruction is computationally much less demanding than for the flat minimum in the case of the extremely weak reconstruction of the Si-terminated SiC(001)-(2×1) surface. The dimer bond length of $d_1=1.74$ Å, as obtained in the empirical calculations by Mehandru and Anderson,[19] is at variance with our results.

TABLE II. Calculated structure parameters for the C-terminated dimer row reconstruction of the β-SiC(001)-(2×1) surface (for their definition, see Fig. 6) as resulting from our work in comparison with other theoretical results from the literature.

C-terminated (2×1) dimers	This work	Craig and Smith [a]	Mehandru and Anderson [b]
d_1 (Å)	1.36	1.36	1.74
d_2 (Å)	1.86	1.86	
d_3 (Å)	1.86	1.86	

[a]Reference 18.
[b]Reference 19.

In Fig. 7 we show the surface band structure of the ideal and the (2×1)-reconstructed dimer row configuration of the C-terminated β-SiC(001) surface. The surface band structure of the ideal surface has been backfolded onto the (2×1) SBZ. It also shows two dangling-bond (D) and two bridge-bond (Br) bands (see the top panels of Fig. 2 for comparison). But now these bands strongly overlap in energy so that the ideal C-terminated SiC(001) surface is metallic. The energetic overlap of the D and Br bands is even more pronounced than for the ideal Si(001) surface (see upper right panel of Fig. 2). The (2×1) dimer row reconstruction leads to a surface band structure that is weakly metallic (see right panel of Fig. 7). A number of salient bands of localized surface states occur. Below the PBS we find at the reconstructed surface a pronounced band, labeled S, originating from s orbitals on the carbon surface-layer atoms. The P_1 and P_2 bands at the ideal and the P_1' and P_2' bands at the reconstructed surface originate from C-Si backbonds having predominantly p wave function character. In the gap region of the reconstructed surface we find a π and a π^* band, which are very similar to the related bands at the C(001)-(2×1) surface[30] and a P_5' band. The π and π^* bands are separated in energy by roughly 1 eV. They originate from symmetric (π) and antisymmetric (π^*) linear combinations of the dangling-bond orbitals at the two dimer atoms, as can be seen in Fig. 8, where we show charge densities of the π, π^*, and P_5' surface states. The P_5' band (the P_5 band at the ideal surface) originates from p states at the surface-layer C atoms, which are oriented perpendicular to the dimers and parallel to the surface plane (see the bottom panel of Fig. 8). The P_5' band is mostly occupied and, in particular, it closes the gap between the π and π^* bands. Such a P_5' surface state band does not occur at C(001)-(2×1) in the gap energy region.[30] It occurs at C-terminated SiC(001) because the Si atoms at the second layer have a weaker potential than the comparable C atoms at the second layer of C(001)-(2×1), so that this band can move up in energy relative to the PBS

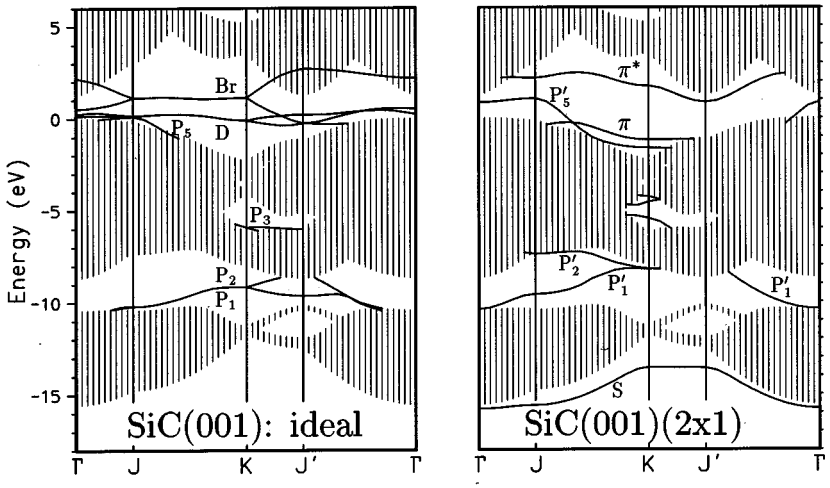

FIG. 7. Surface band structures for the ideal (left panel) and the (2×1) dimer row reconstructed C-terminated surface of β-SiC(001) (see also the caption of Fig. 2).

at the SiC surface. It is this P_5' band that mainly differentiates C-terminated β-SiC(001)-(2×1) from C(001)-(2×1) and that renders the former surface metallic while the latter is semiconducting.[30]

The (2×1) dimer row configuration for the C-terminated surface turns out to be the minimum-energy configuration in our results, as mentioned already. We have chosen this configuration, therefore, as an exemplary case to identify the effects of quasiparticle corrections on the surface band structure of SiC. To this end we have carried out a *GW* quasiparticle surface band structure calculation of C-terminated β-SiC(001)-(2×1) using our formalism as described in detail in Ref. 35. The resulting quasiparticle band structure in the gap energy region is compared in Fig. 9 with the LDA band structure from the right panel of Fig. 7. The static dielectric matrix entering the *GW* calculations has been fully evaluated within the random-phase approximation (RPA) and has been extended to finite frequencies employing a plasmon pole model (for details see Ref. 35). Figure 9 clearly reveals that the quasiparticle band structure of C-terminated β-SiC(001)-(2×1) is semiconducting with an indirect surface gap of 0.9 eV. The projected bulk gap is 2.34 eV, in very close agreement with experiment (see Ref. 36). The π and P_5' bands are hardly changed by the quasiparticle corrections with respect to the top of the related projected valence bands, but the empty π^* band moves up in energy

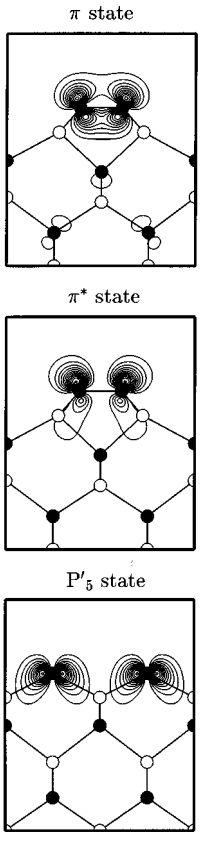

FIG. 8. Charge density contours of salient surface states at the C-terminated β-SiC(001)-(2×1) surface for the dimer row reconstruction. The π and π^* states are shown at the *K* point and the P_5' state is shown at the Γ point of the SBZ (see also the caption of Fig. 3). The former are shown in the *x*-*z* plane containing the dimers while the P_5' state is shown in the *y*-*z* plane.

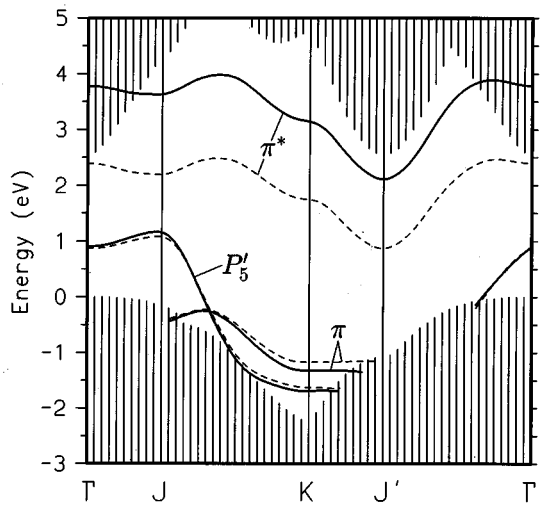

FIG. 9. Section of the surface band structure of the dimer row reconstruction of the C-terminated β-SiC(001)-(2×1) surface [see Fig. 5(b)] as resulting from our LDA (dashed lines) and our quasiparticle GW (full lines) calculations. All bands are referred to their respective valence band maximum, $E_{\mathrm{VBM}}=0$ eV.

TABLE III. Calculated structure parameters for the C-terminated staggered dimer reconstruction of β-SiC(001)-$c(2\times2)$ as resulting from our work in comparison with other theoretical results from the literature. The bond lengths d_1, d_2, and d_3 are defined analogously to those in Table II and Δz_1 (Δz_2) are the vertical distances between the first and second (second and third) layers at the surface.

C-terminated $c(2\times2)$ dimers	This work	Yan *et al.* [a]	Käckell *et al.* [b]	Craig and Smith [c]
d_1 (Å)	1.36	1.39	1.38	1.37
d_2 (Å)	1.93	1.91		1.91
d_3 (Å)	1.93	1.91		1.91
Δz_1 (Å)	0.80	0.79	0.79	0.64
Δz_2 (Å)	1.14	1.12		1.16

[a]Reference 14.
[b]Reference 15.
[c]Reference 18.

almost rigidly by some 1.3 eV, opening up the gap. The effects of the quasiparticle corrections, in general, are thus very similar at this surface to those at other semiconductor surfaces like Si(001)-(2×1) (see, e.g., Ref. 35).

2. c(2×2) staggered dimer structure

Next we have investigated the $c(2\times2)$ staggered C dimer configuration as shown in Fig. 5(c). In this case the atoms on the topmost four layers in the supercell were allowed to move in all three Cartesian directions. The resulting local bonding configuration of the C surface dimers is very similar to that of the (2×1) dimer row configuration [cf. Figs. 5(b) and 5(c)]. Again we end up with symmetric C dimers with a dimer bond length of 1.36 Å. Thus again C═C double bonds are formed. Our optimal structure parameters for the $c(2\times2)$ staggered dimer structure are compared in Table III with other theoretical results from the literature. For this C-terminated surface structure also the general agreement among the different results is very close in spite of some slight differences in detail. Again this is a case of a very strong reconstruction, which is found equally well as a local minimum in $E_{\rm tot}$ by different *ab initio* and semiempirical schemes. In our results the (2×1) dimer row reconstruction [Fig. 5(b)] is lower in energy by $\Delta E=0.15$ eV per unit cell than the staggered dimer configuration (see Table IV). It should be noted, however, that this energy difference is very small as compared to the energy gain of $E_{\rm rec}=4.88$ eV that distinguishes the ideal from the (2×1)-reconstructed dimer row configuration. In contrast to our result, Craig and Smith[18] find the staggered $c(2\times2)$ dimer configuration to be *lower* in energy by $\Delta E=0.79$ eV per dimer as compared to the (2×1) dimer row structure.

The surface band structure of the $c(2\times2)$ staggered dimer reconstruction is shown in Fig. 10. The irreducible part of the $c(2\times2)$ SBZ (one-quarter of the full zone) is shown as an inset where the labeling of high-symmetry points as used in this paper is introduced. The surface bands for this configuration are very similar, in general, to those of the (2×1) dimer row configuration (see Fig. 7, for comparison). The topology of the band structure, of course, is different because of the change in the SBZ. This staggered $c(2\times2)$ configuration also gives rise to a metallic surface within the LDA. The charge densities of the π, π^*, and P_5' states are very similar to those in Fig. 8, and are not shown as a separate figure, therefore.

TABLE IV. Calculated energy gains $E_{\rm rec}$ per (2×1) unit cell (in eV) for four different reconstructions of the C-terminated β-SiC(001) surface in comparison with other theoretical results from the literature. The absolute energy gain $E_{\rm rec}=E_{2\times1}$ due to the (2×1) dimer row reconstruction was not explicitly given in Ref. 18 but the energy gains due to the $c(2\times2)$ reconstructions were given relative to $E_{2\times1}$.

Structure	$E_{\rm rec}$ (eV) per (2×1) unit cell: This work	Käckell *et al.* [a]	Yan *et al.* [b]	Craig and Smith [c]
(2×1)				
Dimer rows	-4.88			$E_{2\times1}$
(1×2)				
C_2 group rows	-4.58			
$c(2\times2)$				
Staggered dimers	-4.73	-4.360	-3.0	$E_{2\times1}-0.79$
Staggered C_2 groups	-4.76	-4.356	-3.6	$E_{2\times1}+0.97$

[a]Reference 15.
[b]Reference 14.
[c]Reference 18.

3. c(2×2) staggered C_2 group structure

Powers *et al.*[11] have favored a $c(2\times2)$ staggered C_2 group configuration on the basis of their tensor LEED data.

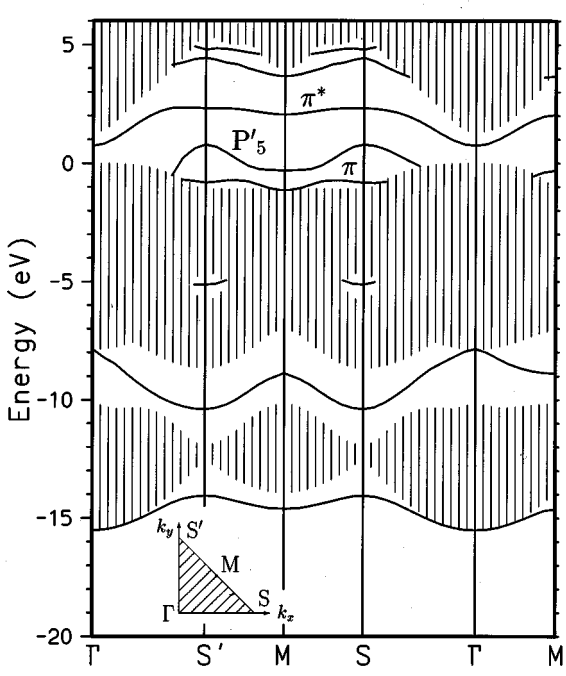

FIG. 10. Surface band structure of the C-terminated staggered dimer configuration of the β-SiC(001)-$c(2\times2)$ surface [see Fig. 5(c)]. The inset shows the irreducible part of the SBZ (one-quarter of the full SBZ).

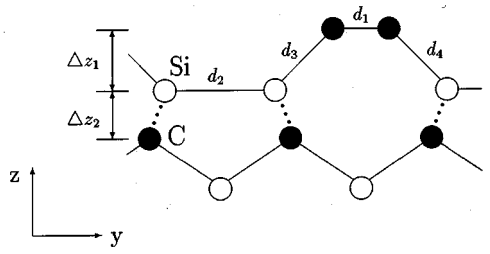

FIG. 11. Side view of the basic structural unit of the staggered C_2 group reconstruction of the C-terminated β-SiC(001)-$c(2\times2)$ surface [see also Fig. 5(d)]. The nomenclature for the structural parameters given in Table V is introduced.

We have, therefore, energy-optimized such a structure, as well. Our result is shown in Fig. 5(d). The bond length in these C_2 groups turns out to be 1.22 Å, a value which is characteristic for C≡C triple bonds.[37] The Si sublayer atoms relax in this structure into weakly bonded dimers with a bond length of 2.40 Å. A side view of our optimized structure, introducing the structural parameters, is shown in Fig. 11. Our optimal structure parameters are compared in Table V with *ab initio* results of Yan, Smith, and Jónsson[14] and of Käckell, Furthmüller, and Bechstedt.[15] Again the results of the different calculations are in very close general agreement. In our results this structure is lower in energy by only $\Delta E=0.03$ eV per unit cell relative to the staggered dimer arrangement (see Table IV), while Yan, Smith, and Jónsson[14] obtain a larger energy gain of about $\Delta E=0.6$ eV between these two configurations. In marked contrast to these *ab initio* results, Craig and Smith[18] find this staggered configuration of triple-bonded C_2 groups *less favorable* by $\Delta E=1.76$ eV with respect to the $c(2\times2)$ staggered dimer configuration (see Table IV).

Interestingly enough, the $c(2\times2)$ C_2 group configuration gives rise to a semiconducting surface already in the LDA, as opposed to the (2×1) dimer row and $c(2\times2)$ staggered dimer configurations. A relevant section of the respective surface band structure, given in Fig. 12, exhibits a gap energy of $E_g=1.28$ eV. It can be expected that a *GW* calculation for this configuration would simply open up the surface gap even further. The band structure shows only a few bands of localized surface states which are close to the PBS. These findings are in good general agreement with photoemission

TABLE V. Calculated structural parameters for the C-terminated C_2 group reconstruction of the β-SiC(001)-$c(2\times2)$ surface (for their definition, see Fig. 11) in comparison with other theoretical results from the literature.

C-terminated $c(2\times2)$ C_2 groups	This work	Yan *et al.* [a]	Käckell *et al.* [b]
d_1 (Å)	1.22	1.22	1.23
d_2 (Å)	2.40	2.38	2.38
d_3 (Å)	1.83	1.87	1.82
d_4 (Å)	1.83	1.87	1.82
Δz_1 (Å)	1.32	1.30	
Δz_2 (Å)	1.04	1.02	

[a]Reference 14.
[b]Reference 15.

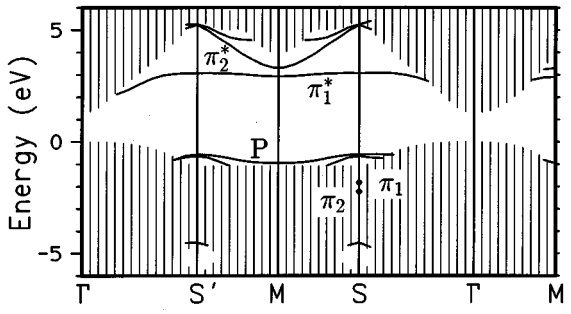

FIG. 12. Section of the surface band structure of the staggered C_2 group reconstruction of the C-terminated β-SiC(001)-$c(2\times2)$ surface [see Fig. 5(d)]. For the labeling of high-symmetry points of the SBZ, see the inset of Fig. 10. The π_1 and π_2 resonances are pronounced at the *S* point of the SBZ only.

measurements carried out for $c(2\times2)$-reconstructed surfaces by Bermudez and Long[38] and by Semond *et al.*,[39] who do not observe surface states in the gap energy region. Charge densities of characteristic surface states, presented in Fig. 13, show that these states originate from the C_2 groups at the surface, as well as from the Si dimers at the second layer. The π_1^* and π_1 states are antibonding and bonding states of the triple-bonded C_2 groups and they strongly resemble the π^* and π states in Fig. 8. The *P* state originates from p_y and p_z orbitals at the C_2 groups and the second-layer Si dimers. The π_2 state lies in the surface plane and is a bonding state related to the C_2 surface groups. Both π_1 and π_2 states reside within the PBS (see Fig. 12) because of the very strong triple bond in the C_2 groups. The π_1^* and π_2^* bands are the antibonding partners of the π_1 and π_2 bonding states.

4. (1×2) C_2 group row structure

To complete our systematic study, we have finally investigated the C_2 group row (1×2) structure as shown in Fig.

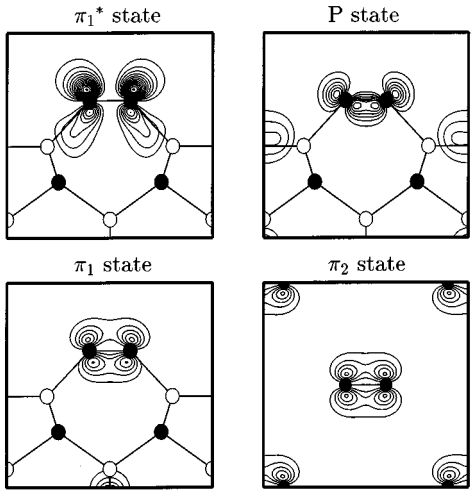

FIG. 13. Charge density contours of salient surface states at the *S* point of the SBZ of the staggered C_2 group reconstructed C-terminated β-SiC(001)-$c(2\times2)$ surface. The states π_1, π_1^*, and *P* are drawn in the *y*-*z* plane perpendicular to the surface containing the C_2 groups, while the π_2 state is shown in the *y*-*x* surface plane.

5(e). It also leads to a local minimum of the total energy in configuration space. The local bonding of the C_2 groups in this configuration is practically identical to that of the staggered C_2 groups in Fig. 5(d). The bond length in the C_2 groups is 1.22 Å in this case, as well. The sublayer Si atoms form symmetric Si dimers with a bond length of 2.39 Å. As shown in Table IV, this configuration is $\Delta E = 0.18$ eV higher in energy than the $c(2\times2)$ staggered C_2 group configuration. We refrain from showing the surface band structure of this configuration since it is favored neither by experiment nor by theory as the optimal configuration.

5. Comparison with experimental data

Powers *et al.*[11] have observed two quantitatively different (2×2) configurations of the C-terminated surface depending sensitively on the surface preparation method used. Exposing the SiC(001)-(2×1) surface to ethylene gas (C_2H_4), they arrive at a bond length of 1.25 Å between the surface carbon atoms in the C_2 groups. In this case the Si sublayer atoms seem to remain nearly in bulklike positions, not forming Si dimers. When the authors[11] prepare the $c(2\times2)$ surface by annealing of SiC(001)-(2×1), the C atoms form C_2 groups with a bond length of 1.31 Å. In this case the second-layer Si atoms have a bond length of 2.71 Å which is considerably smaller than the ideal second-neighbor distance of 3.08 Å. These experimental results are understandable in view of our theoretical results which show very small energy differences between the different (2×1), (1×2), and $c(2\times2)$ structures (see Table IV) but an extremely large energy difference between the ideal and all considered reconstructed configurations. It is thus conceivable that domains of competing local reconstructions of the different types discussed above can coexist at the same sample surface depending on the particular preparation method used and on the local atomic composition, as was observed in experiment.[10,11]

In conclusion of Sec. III B, we can state that our structure optimization slightly favors the (2×1) C dimer row reconstruction, while experiment seems to favor the $c(2\times2)$ staggered C_2 group reconstruction. These structural results should be interpreted in view of the fact that the energy differences between the different investigated structures are smaller than or equal to 0.3 eV per unit cell, only (see Table IV). Concerning the electronic structure, we find that the quasiparticle surface band structure of the (2×1) dimer row model is semiconducting with an indirect gap of 0.9 eV. For the $c(2\times2)$ staggered C_2 group reconstruction the LDA surface band structure already shows a direct gap of 1.28 eV, which is the projected bulk gap, and it is to be expected, therefore, that the equivalent quasiparticle surface gap will be given by the quasiparticle bulk gap. Both in experiment[38,39] and in our theoretical results there are no localized surface states in the gap of the $c(2\times2)$ staggered C_2 group reconstruction. Since the energy difference between the (2×1) dimer row and the $c(2\times2)$ staggered C_2 group models turns out to be only 0.12 eV per (2×1) unit cell in our results, and since the actual structure of the C-terminated surface is sensitively dependent on the surface preparation, one can expect that more detailed work is needed in this area to resolve the remaining small quantitative discrepancies.

IV. SUMMARY

We have presented *ab initio* calculations for a variety of (2×1)- and $c(2\times2)$-reconstructed β-SiC(001) surfaces. Total-energy-minimization calculations have been carried out to determine optimal surface atomic configurations. The Si-terminated (2×1) reconstruction shows only slight displacements of the Si surface-layer atoms with a bond length of 2.73 Å and an energy gain of 0.01 eV. This reconstruction behavior was unexpected in view of the strong asymmetric dimer reconstruction of the Si(001)-(2×1) surface. We have scrutinized the origins of this strikingly different reconstruction behavior and have given a number of physical reasons for its occurrence. Our surface electronic structure for this surface is semiconducting. At the C-terminated (2×1)-reconstructed surface we find as optimal configuration a symmetric C═C dimer row reconstruction with an energy gain of 4.88 eV. The surface carbon atoms form double bonds with a bond length of 1.36 Å very similar to that in C_2H_4 molecules and at the C(001)-(2×1) surface. The LDA band structure for this energetically optimal configuration is found to be metallic. The respective quasiparticle band structure evaluated within the *GW* approximation employing the full RPA dielectric matrix, however, is semiconducting with an indirect gap of 0.9 eV. Since experiment favors $c(2\times2)$ configurations for the C-terminated surface, we have also energy-optimized a $c(2\times2)$ staggered dimer model and two models involving triple-bonded C_2 groups. The $c(2\times2)$ staggered dimer model yields double-bonded C═C dimers with a bond length of 1.36 Å, while both C_2 group models yield triple-bonded C_2 groups in bridge positions above the sublayer Si atoms which form symmetric dimers themselves. The bond lengths of the C_2 groups and of the sublayer Si dimers are 1.22 and 2.40 Å in the $c(2\times2)$ staggered C_2 group and 1.22 and 2.39 Å in the (1×2) C_2 group row configurations, respectively. For the $c(2\times2)$ staggered C_2 group model the LDA surface band structure exhibits a direct gap of 1.28 eV and it is to be expected that the related quasiparticle surface band structure gap will be equal to the quasiparticle bulk gap. Thus also this model is semiconducting. The energy differences among the four C-terminated surfaces investigated are very small (less than or equal to 0.3 eV) as compared to the very large energy gain of more than 4.5 eV per (2×1) unit cell that is observed for each reconstructed surface relative to the ideal (1×1) surface. On the basis of these findings, coexistence of local domains of different reconstructions at the C-terminated surface is conceivable, a fact which might complicate an unequivocal surface structure determination in experiment. Our results of the C-terminated surfaces are in close general agreement with all other calculations and with experiment, although our results favor the (2×1) C═C dimer row over the experimentally preferred $c(2\times2)$ staggered C_2 group reconstruction by 0.12 eV. Our results for the Si-terminated surface are in close agreement with the results of a complementary *ab initio* calculation but they are in contradiction to experiment and to other calculations. The discrepancy between the experimentally determined structure and our optimized structure for this surface is very pronounced. More experimental work could be helpful to resolve the issue. In particular, it would be most helpful if Si-

as well as C-terminated samples could be grown with very good lateral long-range order and studied by angle-resolved photoemission spectroscopy and scanning tunneling microscopy or spectroscopy. Certainly, this would yield a wealth of information not only on structural but also on electronic properties, which could be compared with our results. Since the electronic properties of the different structural models optimized in our calculations are distinctly different, such comparisons could be very revealing. We are looking forward to further experimental studies of polar β-SiC(001) surfaces and we hope that our results, many of which are predictions, will stimulate such future work.

Note added in proof. Finally, we mention that our results for the staggered C_2 group β-SiG(001)-$c(2\times2)$ structure are in excellent agreement with the most recent NEXAFS results obtained by J. P. Long, V. M. Bermudez, and D. E. Ramaher [Phys. Rev. Lett. **76**, 991 (1996)].

ACKNOWLEDGMENTS

One of us (M.S.) would like to acknowledge support by the Bischöfliche Studienförderung Cusanuswerk (Bonn, Germany). In particular it is our pleasure to acknowledge a fruitful exchange of ideas and unpublished results with Professor H. Jónsson and Dr. A.P. Smith from the University of Washington at Seattle.

[1] R. F. Davis, Z. Sitar, B. E. Williams, H. S. Kong, H. J. Kim, J. W. Palmour, J. A. Edmond, J. Ryu, J. T. Glass, and C. H. Carter, Jr., Mater. Sci. Eng. B **1**, 77 (1988).

[2] W. J. Choyke, in *The Physics and Chemistry of Carbides, Nitrides and Borides*, Vol. 183 of *NATO Advanced Study Institute, Series E: Applied Sciences*, edited by R. Freer (Kluwer, Dordrecht, 1990), p. 563.

[3] G. Pensl and R. Helbig, in *Festkörperprobleme, Advances in Solid State Physics*, edited by U. Rössler (Vieweg, Braunschweig, 1990), Vol. 30, p. 133.

[4] A. Garcia and M. L. Cohen, Phys. Rev. B **47**, 4215 (1993); **47**, 4221 (1993).

[5] M. Sabisch, P. Krüger, and J. Pollmann, Phys. Rev. B **51**, 13 367 (1995).

[6] M. Dayan, J. Vac. Sci. Technol. A **4**, 38 (1986).

[7] R. Kaplan, Surf. Sci. **215**, 111 (1989).

[8] S. Hara, W. F. J. Slijkerman, J. F. van der Veen, I. Ohdomari, S. Misawa, E. Sakuma, and S. Yoshida, Surf. Sci. Lett. **231**, L196 (1990).

[9] T. M. Parill and Y. W. Chung, Surf. Sci. **243**, 96 (1991).

[10] V. M. Bermudez and R. Kaplan, Phys. Rev. B **44**, 11 149 (1991).

[11] J. M. Powers, A. Wander, P. J. Rous, M. A. van Hove, and G. A. Somorjai, Phys. Rev. B **44**, 11 159 (1991).

[12] J. M. Powers, A. Wander, M. A. van Hove, and G. A. Somorjai, Surf. Sci. Lett. **260**, L7 (1992).

[13] S. Hara, S. Misawa, S. Yoshida, and Y. Aoyagi, Phys Rev. B **50**, 4548 (1994).

[14] H. Yan, A. P. Smith, and H. Jónsson, Surf. Sci. **330**, 265 (1995).

[15] P. Käckell, J. Furthmüller, and F. Bechstedt, in Proceedings of the Fifth International Conference on the Formation of Semiconductor Interfaces, Princeton, NJ, 1995 [Appl. Surf. Sci. (to be published)]; and Surf. Sci. (to be published).

[16] J. Pollmann, P. Krüger, M. Rohlfing, M. Sabisch, and D. Vogel, in Proceedings of the Fifth International Conference on the Formation of Semiconductor Interfaces, Princeton, NJ, 1995 [Appl. Surf. Sci. (to be published)].

[17] B. I. Craig and P. V. Smith, Surf. Sci. **233**, 255 (1990).

[18] B. I. Craig and P. V. Smith, Surf. Sci. Lett. **256**, L609 (1991).

[19] S. P. Mehandru and A. B. Anderson, Phys. Rev. B **42**, 9040 (1990).

[20] P. Badziag, Surf. Sci. **269-270**, 1152 (1992).

[21] P. Hohenberg and W. Kohn, Phys. Rev. **136**, B864 (1964); W. Kohn and L. J. Sham, *ibid.* **140**, A1133 (1965).

[22] D. M. Ceperley and B. J. Alder, Phys. Rev. Lett. **45**, 566 (1980).

[23] J. P. Perdew and A. Zunger, Phys. Rev. B **23**, 5048 (1981).

[24] L. Kleinman and D. M. Bylander, Phys. Rev. Lett. **48**, 1425 (1982).

[25] M. Sabisch, Diploma thesis, Universität Münster, 1993.

[26] D. R. Hamann, M. Schlüter, and C. Chiang, Phys. Rev. Lett. **43**, 1494 (1979); Phys. Rev. B **32**, 393 (1984); D. Hamann, *ibid.* **40**, 2980 (1989).

[27] J. Ihm, A. Zunger, and M. L. Cohen, J. Phys. C **12**, 4409 (1979).

[28] C. G. Broyden, Math. Comput. **19**, 577 (1965); see also D. D. Johnson, Phys. Rev. B **38**, 12 807 (1988).

[29] M. Scheffler, J. P. Vigneron, and G. Bachelet, Phys. Rev. B **31**, 6541 (1985); P. Krüger and J. Pollmann, Physica B **172**, 155 (1991).

[30] P. Krüger and J. Pollmann, Phys. Rev. Lett. **74**, 1155 (1995).

[31] A. Ramstad, G. Brocks, and P. J. Kelly, Phys. Rev. B **51**, 14 504 (1995).

[32] E. L. Bullock, R. Gunnella, L. Patthey, T. Abukawa, S. Kono, C. R. Natoli, and L. S. O. Johansson, Phys. Rev. Lett. **74**, 2756 (1995).

[33] A. P. Smith and H. Jónsson (private communication).

[34] A. F. Wells, *Structural Inorganic Chemistry* (Clarendon, Oxford, 1975).

[35] M. Rohlfing, P. Krüger, and J. Pollmann, Phys. Rev. B **52**, 1905 (1995).

[36] M. Rohlfing, P. Krüger, and J. Pollmann, Phys. Rev. B **48**, 17 791 (1993).

[37] A. F. Wolkenstein, *Struktur und physikalische Eigenschaften der Moleküle* (Teubner Verlagsgesellschaft, Leipzig, 1960).

[38] V. M. Bermudez and J. P. Long, Appl. Phys. Lett. **66**, 475 (1995).

[39] F. Semond, P. Soukiassian, P. S. Mangat, and L. di Ciaccio, J. Vac. Sci. Technol. B **13**, 1591 (1995).